Semi-Annual Report to

National Aeronautics and Space Administration

Ames Research Center
Moffett Field, California 94035

Ultrasonic Doppler Measurement of Renal Artery Blood Flow

Grant Number NGR-05-020-615

Submitted by

Integrated Circuits Laboratory
Stanford Electronics Laboratories
Stanford University
Stanford, California

July 1974

ABSTRACT

Implantable pulsed-Doppler ultrasonic flowmeter development has resulted in designs for application to the aortas of dogs and humans, and to human renal and coronary arteries. A figure of merit has been derived for each design, indicating the degree of its precision.

An H-array design for transcutaneous observation of blood flow has been developed and tested in vitro. Two other simplified designs for the same purpose obviate the need to determine vessel orientation. One of these will be developed in the next time period.

Techniques for intraoperative use and for implantation have had mixed success. While satisfactory on large vessels, higher ultrasonic frequencies and alteration of transducer design are required for satisfactory operation of pulsed Doppler flowmeters with small vessels.

CONTENTS

I. INTRODUCTION

This semi-annual report covers the period from September 1, 1973, through February 28, 1974. It discusses recent developments in work toward achievement of satisfactory blood flowmeters suitable for measuring flow in the renal artery, both with implantable devices and with external devices operating transcutaneously. The use of custom integrated circuits and ultrasound are essential to accomplish this task in the approach described here.

Implantable devices are essential to permit unhampered observation of blood flow to specific organs in awake, unanesthetized animals. Transcutaneous observations avoid the necessity for invasion of the body in order to measure the flow. Instruments available previously for flow measurement have been less accurate and reliable than those described here.

Determination of renal blood flow in man is considered an important factor in understanding the mechanisms operative in producing the diuresis observed subsequent to weightlessness and bedrest simulation of weightlessness and, therefore, are important in understanding the effects of space flight on man.

Analysis of several system tradeoff considerations has been completed in the development of a pulsed-Doppler ultrasonic blood flowmeter. Included are pulse burst length, repetition frequency, filtering and ultrasonic frequency choice and transducer diameter. These are drawn together into an optimal design procedure and a study made of the performance limitations.

To complement the design development work, implementation techniques are also being developed using dogs to test the effectiveness of the designs as a prelude to their application to people.

II. TECHNICAL RESULTS

A. Implantable Pulsed Flowmeter (R. W. Gill and J. D. Meindl)

Work on the realization of the pulsed flowmeter implantable electronics in integrated-circuit form is continuing. The final circuit configurations have been chosen on the basis of minimum power drain and reliable operation over a wide range of supply voltages. These circuits have now been laid out as integrated circuits, and the IC masks made. Emphasis is, at present, being placed on development of a suitable IC fabrication process, and it is expected that working integrated circuits will be fabricated in the near future. Work is also proceeding on the

wideband telemetry link required for the pulsed flowmeter. This has proved to be a more difficult task than was originally envisioned.

The following discussion is a reproduction of a relevant paper on optimal system design of the pulsed Doppler ultrasonic blood flowmeter presented by the authors at the IEEE 1973 Ultrasonics Symposium held at Monterey, California on November 5, 1973. The work presented here was also supported by the National Institutes of Health under PHS Research Grant No. 1 PO1 GM17940-04.

OPTIMAL SYSTEM DESIGN OF THE PULSED DOPPLER ULTRASONIC BLOOD FLOWMETER

R.W. Gill and J.D. Meindl
Stanford Electronics Laboratories
Stanford, CA 94305

ABSTRACT. The pulsed Doppler blood flowmeter has demonstrated its utility in a number of applications, both clinical and research. The future is certain to see increasing use of this type of flowmeter for several reasons, including its convenience and stability and the unique data it can produce.

In the design of the flowmeter a number of tradeoffs must be made. This paper presents a systematic approach to these tradeoffs, leading to a design procedure which optimizes flowmeter performance for a given set of physiological constraints. Sample designs for typical applications are presented. The particular flowmeter configuration considered is the single-transducer type with the transducer adjacent to the vessel.

This paper deals with the tradeoffs involved in the design of the pulsed Doppler ultrasonic blood flowmeter, and the selection of the various parameters of the flowmeter to optimize its performance subject to the physiological constraints of the application. Specifically, the analysis is applicable to the case of a non-directional[1] or quadrature directional[2] pulsed flowmeter, with a single transmit/receive transducer adjacent to the vessel. The analysis can be modified to deal with an offset directional flowmeter[3], transcutaneous measurement with or without a lens, and the case where separate transmitting and receiving transducers are used.

Optimization of the flowmeter performance is taken to mean obtaining maximum range resolution and flow measurement accuracy subject to the needs for unambiguous measurement of range and velocity. The maximization of the Doppler signal-to-noise ratio for a given transmitted acoustic power is also an important consideration.

A simple first-order theory is developed, since it is desirable to study the design tradeoffs analytically. Thus, for example, the beam pattern of the transducer is modelled by a theory which may deviate significantly from the actual pattern in any given case, and the sample volume of the flowmeter has to be somewhat arbitrarily defined, since the intensity falls off slowly at its edges. In addition, the problems of optimum demodulation of the Doppler signal have been omitted; this subject deserves considerable attention in its own right.

The block diagram of an implantable pulsed flowmeter is shown in Fig. 1, and some typical waveforms in Fig. 2.[4] Only one demodulator channel is shown for convenience. A non-implantable version of this is obtained by eliminating the telemetry link and connecting the video and sync signals directly to the demodulator. Although other pulsed flowmeters differ from this in several respects, the following analysis should still apply to them directly. The parameters which must be determined are: ultrasonic frequency, burst repetition frequency, transducer diameter, transducer angle, burst length, rf amplifier and video amplifier bandwidth, and audio filter cutoff frequencies. The factors influencing the choice of each parameter are discussed, and then a design procedure presented which combines all these considerations to give an optimized flowmeter design. The flowmeter performance and the effects of physiological and transducer constraints on it are then discussed. Finally, some typical designs are presented.

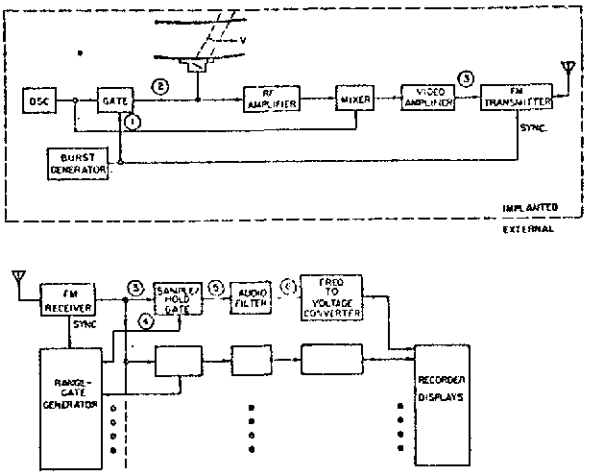

Fig. 1. Pulsed Flowmeter Block Diagram

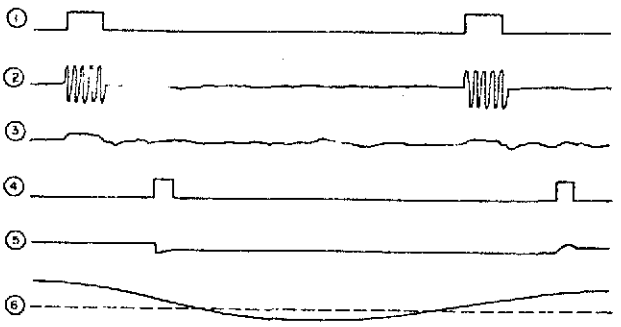

Fig. 2. Typical Flowmeter Waveforms

Burst Length

Fig. 3 shows the beam and vessel geometry and the definition of some terms. The flowmeter resolution (X) is given by the projection of the sample volume (the volume of blood from which significant scattering is received at any one instant) on the vessel diameter. It can be expressed as

$$X = 1/2\ c\ T_{eff} \sin\theta + w \cos\theta \qquad (1)$$

where $c = 1.57 \times 10^5$ cm/sec is the velocity of sound in blood, T_{eff} is the effective burst length and w is the beam width. To maximize resolution T_{eff} must clearly be minimized. It is determined by the length of the drive burst applied to the transducer, and by the bandwidths of the transducer and all the following electronics up to the sample/hold gates. In practice

T_{eff} can be defined as the interval between the -10dB points of the return from a single reflector, measured at the output of the video amplifier.

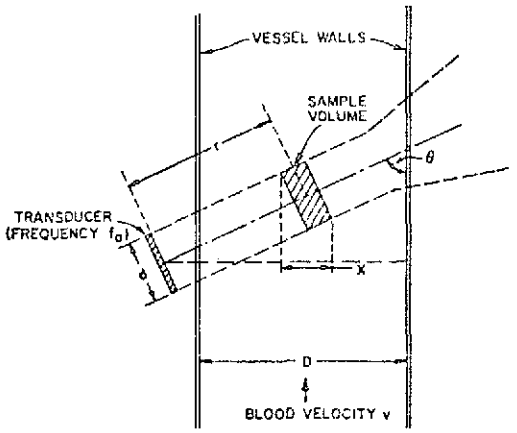

Fig. 3. Beam and Vessel Geometry

The bandwidth of the transducer is given by f_o/Q_t where Q_t is the transducer Q, and f_o is the ultrasonic frequency. The rf amplifier bandwidth is set equal to the transducer bandwidth; a narrower rf bandwidth would degrade resolution, while a broader one would unnecessarily degrade the signal-to-noise ratio.[5] Since the mixer folds the spectrum in half about zero frequency, the video bandwidth is one half the rf bandwidth. The length of the drive burst is made equal to the reciprocal of the transducer bandwidth

$$T = Q_t/f_o \tag{2}$$

since a shorter burst would reduce the power received without significantly improving resolution while a longer one would degrade the resolution. The effective burst length can then be written as

$$T_{eff} = Q_{eff}/f_o \tag{3}$$

where Q_{eff} is the transducer Q modified to account for the effect of the rf and video amplifier bandwidths.

Thus resolution is best for a low Q transducer and high ultrasonic frequency. Typically Q_t may be reduced to about 5 by using a suitable piezoelectric material and acoustic loading and matching layers, giving $Q_{eff} \sim 7$.

Audio Filter

Reflections from vessel walls and other body structures produce large low-frequency Doppler signals which tend to obscure the blood flow information. For this reason a lower cutoff frequency of 100 or 200 Hz is typically chosen. The upper cutoff is chosen to be just above the highest Doppler signal expected, and just below one half of the burst repetition rate. This is because the sampling theorem of communications theory proves that the highest Doppler frequency which can be unambiguously measured is one half of the sampling rate;[6] in practice, filtering requirements reduce the maximum permissible Doppler frequency to about 90% of this value:

$$f_{dmax} = 0.45\ f_r \tag{4}$$

where f_r is the burst repetition rate. Thus, for a given ultrasonic frequency and transducer angle, a limit is set by f_r on the maximum velocity which can be measured, according to the Doppler equation

$$f_d = 2\,\frac{v}{c}\,f_o \cos\theta \tag{5}$$

where f_d is the Doppler shift, v is the blood velocity, c is the velocity of sound and f_o is the ultrasonic frequency.

Burst Repetition Frequency

The above discussion implies that a high repetition frequency is desired to allow the measurement of high velocities. However, the need to measure range unambiguously limits the repetition period to the time taken by sound to travel to the opposite wall of the vessel and back to the transducer. Thus the repetition rate chosen is the highest one compatible with this latter constraint:

$$f_r = \frac{c \sin\theta}{2\,D_{max}} \tag{6}$$

where D_{max} is the maximum vessel diameter expected. Then, from (4), the maximum allowable Doppler frequency is

$$f_{dmax} = 0.225\,\frac{c \sin\theta}{D_{max}} \tag{7}$$

Transducer Angle

Consider a flowmeter being used to measure both velocity and volume flow. The velocity is calculated according to the Doppler equation (5)

$$v = \frac{c\,f_d}{2 f_o \cos\theta} \sim \frac{1}{\cos\theta} \tag{8}$$

To calculate volume flow, the velocity distribution across the vessel is spatially averaged and multiplied by the vessel area, determined from the range of the near and far walls. Thus

$$\bar{v} \sim \frac{1}{\cos\theta} \tag{9}$$

and

$$D = 1/2\ c\ \tau \sin\theta \sim \sin\theta \tag{10}$$

where $\bar{v}$ is the spatially averaged velocity, τ is the time between near and far wall echos, and D is the vessel diameter. The volume flow is then given by

$$q = 1/4\pi\ D^2\ \bar{v} \sim \frac{\sin^2\theta}{\cos\theta} \tag{11}$$

Differentiating (8) and (11) with respect to θ and normalizing, the sensitivity of velocity and volume flow measurements to angle errors are given respectively by

$$\frac{1}{v}\,\frac{dv}{d\theta} = \tan\theta \tag{12}$$

$$\frac{1}{q}\,\frac{dq}{d\theta} = \tan\theta + 2\cot\theta \tag{13}$$

These are plotted in Fig. 4. For velocity measurement θ should be small for maximum accuracy, but for volume flow measurement the sensitivity to angle error is lowest near 60°. Since angle errors of 1° or 2° seem unavoidable, it is essential that θ be chosen to minimize sensitivity to such errors.

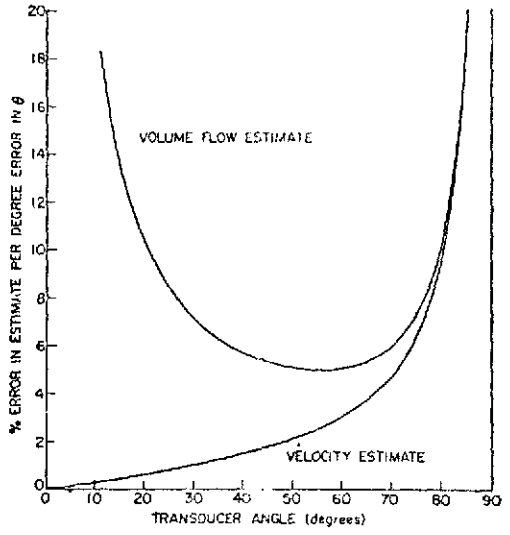

Fig. 4. Velocity and Flow Sensitivities to Angle Error

Other factors which should also be considered in selecting θ are: sample size, maximum range for a given vessel diameter, and the distance travelled along the vessel by the beam as it travels across the vessel. This last factor determines the amount of relatively straight vessel needed to make accurate measurements, which should be minimized, implying that a value of θ near 90° is desirable. The sample size is not strongly dependent on θ for typical burst lengths and transducer size, but it is minimized for $\theta = 90°$. For a given vessel diameter, the maximum range limits the repetition frequency and so the Doppler frequency which can be measured, as given by (7). Again, the range is minimized for $\theta = 90°$, and so a value of θ near 90° is desirable.

The choice of θ is a compromise between all these factors, with the need to minimize the sensitivity to angle errors the dominant consideration. For a flowmeter which is used to measure both velocity and volume flow, a value of 60° is thus normally chosen.

Ultrasonic Frequency

As indicated earlier, and as would be expected intuitively, the ultrasonic frequency should be as high as possible to optimize resolution. However, for a given vessel size there is an upper limit on the Doppler frequency given by (7); for a given velocity this sets an upper limit on the ultrasonic frequency, according to (5). Equating the two upper limits

$$f_{dmax} = 2\,\frac{v_{max}}{c}\,f_o \cos\theta = 0.225\,\frac{c \sin\theta}{D_{max}}$$

$$\text{i.e. } f_o = \frac{c^2 \tan\theta}{8.9 v_{max} D_{max}} \qquad (14)$$

Using this value of the ultrasonic frequency will then maximize the resolution subject to the repetition rate limitation on the Doppler frequency. Equation (14) is plotted in Fig. 5 for a number of vessel diameters and maximum velocities.

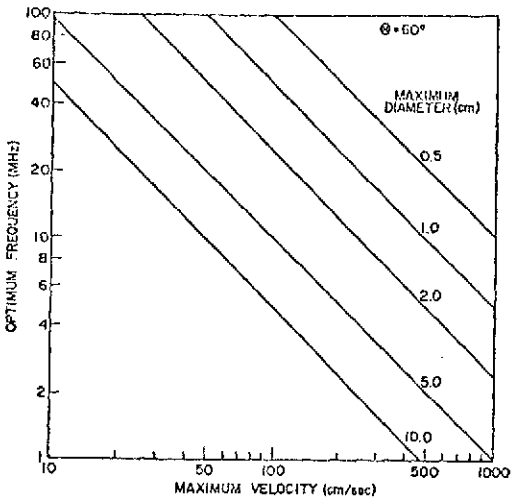

Fig. 5. Frequency for Optimum Resolution as a Function of Vessel Diameter and Maximum Blood Velocity

One further consideration which must be discussed is the variation of signal-to-noise (S/N) ratio with ultrasonic frequency. It will be shown that this is not a critical factor in the choice of f_o.

Consider the scattering from blood at range r. Assume that all the transmitted power is uniformly distributed in a beam of width w, area $(1/4)\pi w^2$. Then the incident power per unit area is given by

$$P_i = \frac{\eta_1 P_t}{(1/4)\pi w^2}\, e^{-a.r} \qquad (15)$$

where P_t is the electrical power delivered to the transducer, η_1 is the transducer transmitting efficiency, and a is the attenuation constant of the intervening medium. For a single target with scattering cross-section A, the scattered power is just $A.P_i$. If the scattering process is first order and independent, as experimental results indicate,[7] the total scattered power is the sum of the powers due to the individual scatters. Thus, it is given by $A.P_i$ multiplied by the number of scatterers in the sample volume. Ignoring the spreading of the burst in time (i.e. assuming $T_{eff} = T$), the scattered power is then

$$P_s = \left[(1/4\,\pi w^2)(1/2\,c\,T)\,n_o\right] A.P_i$$
$$= 1/2\,c\,T n_o A\,\eta_1\,P_t\,e^{-a.r} \qquad (16)$$

using (15), where n_o is the number of scatterers per unit volume. Since the scattering particles are much smaller than the ultrasonic wavelength ($\sim 7\mu$ compared to ~ 0.3mm), the scattering is governed by Rayleigh statistics,[8] and so it may be assumed to be isotropic, with a scattering cross-section given by

$$A = A_o\, f_o^4 \qquad (17)$$

where A is a constant.

The fraction of the scattered power which is received by the transducer is then given by the ratio of the transducer area to the area of a sphere of radius r.

$$P_r = \eta_2\, P_s \left(\frac{\pi d^2}{4}\right)\left(\frac{1}{4\pi r^2}\right)\, e^{-a.r} \qquad (18)$$

where η_2 is the transducer receiving efficiency. Combining equations (16), (17) and (18) gives

$$P_r = \frac{\eta\, c\, T\, n_o\, A_o\, d^2}{32\, r^2} P_t\, f_o^4\, e^{-2a.r} \qquad (19)$$

where $\eta = \eta_1\, \eta_2$ is the overall transducer efficiency.

To make the dependence of the signal-to-noise ratio on f_o explicit, the following relationships are used:

(i) assume Rayleigh scattering, equation (17)

(ii) the attenuation constant (a) is known to be approximately proportional to frequency in the frequency range of interest[9], so

$$a = a_o\, f_o \qquad (20)$$

where a_o is a constant.

(iii) the burst length is given by (2)

(iv) the receiver noise referred to the input can be assumed to be proportional to the receiver bandwidth, i.e.

$$N_r = \frac{N_o\, f_o}{Q_t} \qquad (21)$$

where N_o is the noise per unit bandwidth.

The S/N ratio of the Doppler signal is found by substituting (2) and (20) into (19) and dividing the resulting received power by (21).

$$S/N = \frac{P_r}{N_r} = \frac{\eta\, c\, Q_t^2\, n_o\, A_o\, d^2}{32\, N_o\, r^2} P_t\, f_o^2\, e^{-2a\, f_o r} \qquad (22)$$

The electrical power (P_t) is usually fixed by electronic and/or safety requirements, and the transducer size is determined by resolution requirements. If we assume the transducer Q and efficiency are independent of frequency, then we have

$$S/N \sim \frac{f_o^2}{r^2}\, e^{-2a_o f_o r} \qquad (23)$$

Differentiating this with respect to frequency and setting the derivative equal to zero, the frequency which maximizes the S/N ratio is found to be

$$f_{o\,opt} = \frac{1}{a_o r} \qquad (24)$$

This is plotted in Fig. 6 where r is assumed to be the range to the far wall of the vessel, and a_o is the weighted mean of the attenuation constant for the vessel walls (4dB/cm/MHz) and blood (0.25dB/cm/MHz) assuming a ratio of wall thickness to vessel diameter of 5%.

The shaded area in Fig. 6 indicates the range of frequencies for a given distance (r) for which the S/N ratio is within 3dB of its maximum value. This indicates that a range of frequencies of at least 4:1 is permissible without seriously affecting the S/N ratio. Thus the maximization of S/N ratio is a secondary consideration in the choice of ultrasonic frequency.

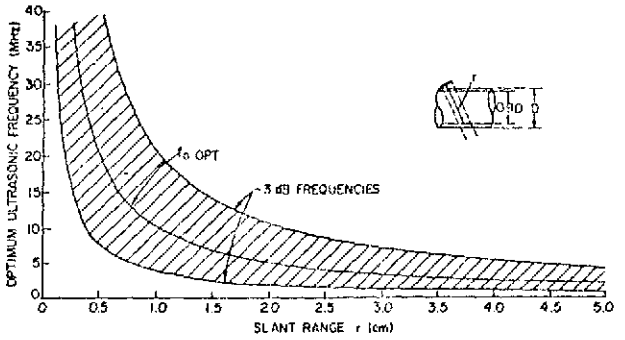

Fig. 6. Optimum Frequency for Maximum S/N ratio

Transducer Diameter

Fig. 7(a) shows the beam envelope for a circular transmitting transducer of diameter d, assuming that it acts as an ideal piston.[9] The axial intensity distribution is shown in Fig. 7(b). Notice that there are a series of maxima and zeros, their exact number being determined by the ratio d/λ where λ is the wavelength; $d/\lambda = 10$ for Fig. 7. The point at which the last axial maximum occurs is conventionally taken as the transition point between the parallel-beam "near field" and the uniformly diverging "far field" where the axial intensity falls off inversely with range. This last maximum occurs approximately at the point

$$r_1 = 0.25\, d^2/\lambda \qquad (25)$$

and this has been used as the definition of the maximum usable range of the transducer.

However, a number of comments are in order. First, the definition of the beam discussed above defines the boundaries as those points at which the intensity falls to zero. A more realistic definition would seem to be the locus of points at which the beam power falls to a certain fraction of its maximum, since the flowmeter demodulator normally has some threshold power level below which it does not detect signal.[10] For example, Fig. 7(c) shows the -6dB beam envelope, again using the "piston" theory.[11] Note that when the receiving sensitivity pattern is also taken into account, the returns from these points are actually 12dB down. The beam width at range r_1 is now less than 1/2 d, and the angle of divergence of the beam in the far field is about 60% of that for the beam of Fig. 7(a). This definition of the beam is not only more optimistic, but also more consistent with the observations of experimenters in the field of ultrasonic imaging.[12]

In addition to the above considerations, Bekker et. al. have demonstrated that the uniform piston assumption is not very realistic, and instead have investigated the cases of a transducer with simply-supported and clamped edges.[13] In both cases the transducer vibration falls to zero at the edges, consistent with observations of actual transducers. Fig. 7(d) shows the axial intensity distribution for the simply-supported transducer for $d/\lambda = 10$; notice that the intensity variation in the near field is much less than for the piston theory, and that the last axial maximum occurs at about $r_1 = 0.19\, d^2/\lambda$. Analysis of the far field indicates that the angle of divergence of the -6dB envelope is

$$\varphi = 0.88\, \lambda/d \qquad (26)$$

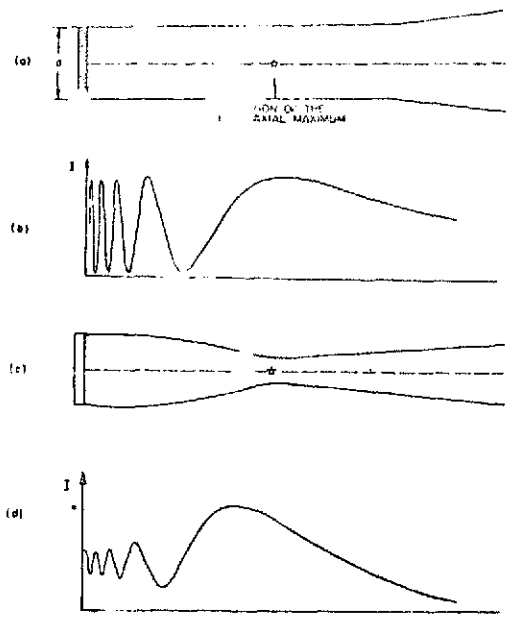

Fig. 7. Transducer Beam Patterns and Axial Intensity Distribution

Defining the maximum usable range of the transducer as the distance at which the -6dB points are 1.5d apart (i.e. the beam width is degraded 50%), equation (26) gives

$$r_{max} = 0.85\ d^2/\lambda$$
$$= 0.85\ d^2 f_o/c \qquad (27)$$

Thus, the transducer is quite useful at ranges up to three times the near field distance given by (25). For a given application, the resolution is maximized if this maximum usable range is set equal to the distance to the far vessel wall; i.e.

$$r_{max} = \frac{D_{max}}{\sin\theta} = \frac{0.85\ d^2 f_o}{c}$$

$$\text{i.e.}\quad d = \left[\frac{1.18\ c\ D_{max}}{f_o \sin\theta}\right]^{1/2} \qquad (28)$$

Optimal Design Procedure

The above considerations can now be drawn together to provide a logical sequence of design steps which optimize the flowmeter performance within the limitations of the physiological situation and transducer parameters. The steps are described below:

(1) Choose θ, the transducer angle. Normally $\theta = 60°$.

(2) From the maximum vessel-size expected, the repetition-rate is calculated from (6), ensuring unambiguous range measurement.

(3) This sets a limit on the highest Doppler signal, according to eq. (7). Choose the highest ultrasonic frequency compatible with this, according to eq. (14) or Fig. 5. This ensures maximum resolution subject to the need for unambiguous velocity measurement. Check to see if the S/N ratio is adequate.

(4) Choose the smallest transducer compatible with the maximum range required. Substituting eq. (14) into (28) gives

$$d = \left[\frac{10\ D_{max}^2\ v_{max}}{c \sin\theta \tan\theta}\right]^{1/2} \qquad (29)$$

(5) The burst length and bandwidths are chosen as discussed above.

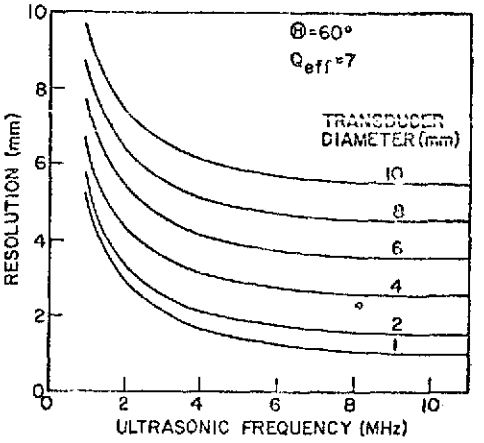

Fig. 8. Flowmeter Resolution as a Function of Frequency and Transducer Diameter

Performance Limitations

The flowmeter resolution is plotted in Fig. 8 as a function of frequency and transducer size, assuming a parallel beam of width d for simplicity. Notice, however, that the design procedure allows the ultrasonic frequency to be expressed in terms of v_{max} and D_{max}, the physiological constraints, according to eq. 14. When this is taken into account, the resolution can be written as

$$X = D_{max}\left[(8.9\ Q_{eff}\ \frac{v_{max}}{c}\cos\theta) + \cot\theta\ (10\ \frac{v_{max}}{c}\cos\theta)^{1/2}\right] \qquad (30)$$

Thus the ratio D_{max}/X, roughly speaking the number of independent samples resolvable across the vessel, is a function only of the maximum velocity expected, the transducer Q, and the transducer angle. This function is plotted in Fig. 9 for θ=60°. Together with the angle-sensitivity curves of Fig. 4, this is probably the most important fundamental limit on flowmeter performance. Other limits are either built into the design (the maximum velocity and vessel diameter) or not fundamental (the S/N ratio can be improved by increasing the transmitted power or improving the processing circuits).

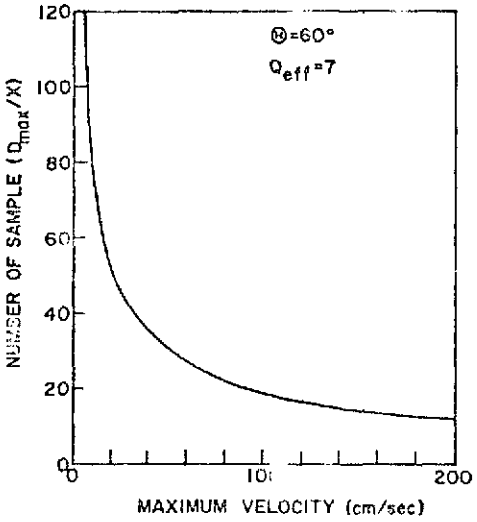

Fig. 9. Number of Samples Across Vessel as a Function of Maximum Blood Velocity.

Conclusion

Table 1 presents some sample flowmeter designs for a variety of applications. It is interesting to note that the designs for the large vessels are very similar to those already used, and also that the figure of merit (the number of independent samples) is quite reasonable.

In summary, the factors influencing the choice of the major flowmeter parameters have been discussed, and a design procedure developed which optimizes the flowmeter performance for a given physiological situation. The flowmeter performance is then specified, and its dependence on the physiological parameters and the transducer properties is explicitly stated.

References

1. Baker D.W., Watkins D.W., "A Phase Coherent Pulse Doppler System for Cardiovascular Measurements," Proc. 20th Ann. Conf. on Engng. in Med. and Biol., 1967.
2. McLeod F.D., "Directional Doppler Demodulation," Proc. 20th Ann. Conf. on Engng. in Med. and Biol., 1967.
3. Haase W.C., Foletta W.S., Meindl J.D., "A Directional Ratiometric Ultrasonic Blood Flowmeter," Proc. IEEE Ultrasonics Symp., 1973.
4. Gill R.W., Brody W.R., Meindl J.D., Angell W.W., "The Pulsed Doppler Ultrasonic Blood Flowmeter and its Applications in Open Heart Surgery," Proc. 2nd World Congress on Ultrasonics in Medicine, 1973.
5. Brody W.R., "Theoretical Analysis of the Ultrasonic Blood Flowmeter," Ph.D. thesis and Technical Report No. 4958-1, Stanford Electronics Laboratory, Stanford University, 1971.
6. Bracewell R., "The Fourier Transform and Its Applications," McGraw-Hill, 1965.
7. Reid J.R., "The Scattering of Ultrasound by Human Blood," Proc 8th Int. Conf. on Med. and Biol. Engng., 1969.
8. Huerter T.F., Bolt R.H., "Sonics" John Wiley and Sons, New York, 1955.
9. Wells P.N.T., "Physical Principles of Ultrasonic Diagnosis," Academic Press, London, 1969.
10. Haase W.C., private communication
11. Zemanek J., "Beam Behavior within the Near Field of a Vibrating Piston," J. Acoust. Soc. Am., 1971.
12. Kossoff G., Robinson D.E., Garrett W.J., "Ultrasonic Two-Dimensional Visualization for Medical Diagnosis," J. Acoust. Soc. Am., 1968.
13. Dekker D.L., Piziali R.L., Dong E., to be published.

Table I

SAMPLE DESIGNS

VESSEL	dog aorta	human aorta	human ren.art.	human cor.art.	Units
MAX. DIAMETER	2.0	4.2	0.9	0.3	cm
MAX. VELOCITY	200	150	65	200	cm/sec
TRANSDUCER ANGLE	60	60	60	60	degrees
BURST REP. FREQ.	34	16.2	76	226	kHz
ULTRASONIC FREQ.	12.1	7.7	83	81	MHz
TRANSDUCER DIAM.	1.8	3.4	0.5	0.3	mm
SAMPLE SIZE	1.7	2.9	0.4	0.3	mm
FIGURE OF MERIT	11.7	14.4	25.6	11.7	
OPTIMUM f_c FOR S/N	4.3	2.2	9.6	29	MHz

B. Transcutaneous Flowmeters

1. Arterial Visualization System (C.F. Hottinger)

The goal of the transcutaneous blood flowmeter project is development of an ultrasonic system capable of quantitative measurement of instantaneous flow through the renal artery. To perform this measurement, the transcutaneous system must be capable of real-time visualization of the effective vessel lumen. The arterial visualization system currently under development generates one or more Doppler B-scans. Sensitive only to moving targets, each scan displays the projection of the effective lumen area onto a reference plane.

An appropriate choice of reference planes permits an unambiguous determination of effective vessel size and orientation. For this reason an H-shaped configuration of linear transducer arrays has been developed; when the H-array is aligned over the vessel axis, the vessel size and orientation can be estimated reliably. A separate transducer element, not part of the visualization system, can then be used with any of several pulsed Doppler demodulator schemes to make a reliable quantitative measurement of flow in real time.

The H-array configuration has been implemented in an assembly involving 78 transducer elements, with center-to-center element spacing as close as 1 mm. Element spacings in this range give the type of near-field resolution acceptable with the larger arteries; closer spacing will achieve the resolution appropriate to the renal artery. In addition, high voltage multiplex circuitry was introduced to permit the higher transmit levels needed for transcutaneous scanning.

The Doppler B-scans indicate the points under the arrays returning total Doppler-shifted audio power above a pre-set threshold. Even when this flow-velocity vector has no component in the direction of the scanning transducers, Doppler shifted audio power is detected. Such mechanisms as beam spread, finite transit time, and flow turbulence contribute to the apparent Doppler shift.

The low power levels involved, however, prompted consideration of other array configurations that avoid perpendicular scanning of the velocity vector. Two new configurations, differing radically from the H-array, have been developed. Both new systems combine a first-moment processor (discussed below) with the Doppler imaging processor in a new configuration to simplify greatly and increase the accuracy of

ultrasonic volume flow measurement. Described as performing a "canonical" measurement of the flow, the method consists of breaking up an arbitrary plane of incremental areas. The incremental flows across these areas are summed to find the entire volume flow. Therefore, no assumptions regarding orientation, turbulence, or velocity profile are necessary to estimate reliably the total flow.

The significance of the canonical method lies in its solution, in concept, of the problem of flow measurement for a large number of the vessels of interest in the body. In the coming year, the simpler of the two canonical methods will be implemented. Involving a single linear array for visualization, as well as a uniform illumination transducer for first-moment detection, the technique promises to be useful both for transcutaneous and intraoperative measurements. Initial tests with arterial models and in vitro specimens will provide a basis for meaningful in vivo measurements later.

Further details of this development are given in the following reproduction of a paper presented at the 1973 IEEE Ultrasonics Symposium held at Monterey, California on November 5, 1973.

AN ULTRASONIC SCANNING SYSTEM FOR ARTERIAL IMAGING

C.F. Hottinger and J.D. Meindl
Department of Electrical Engineering
Stanford University
Stanford, California 94305

ABSTRACT. A transcutaneous system for real-time imaging of arteries is described. A transducer probe containing three linear arrays of elements scans tissues within the element Fresnel zones. Each element is multiplexed in turn to a pulsed Doppler processor to permit real-time visualizations of moving targets. Applications of the motion-indicating B-scans are discussed, with special attention to problems in transcutaneous measurement of blood flow.

A transcutaneous Doppler imaging system has been developed to display real-time visualizations of some of the larger peripheral arteries and veins. The probe for this ultrasonic imaging system consists of an array of pulsed transducer elements, each scanning tissues within the element Fresnel zones. A pulsed Doppler processor is demultiplexed to each of the transducer elements in turn to achieve real-time displays of moving targets and suppression of stationary target displays.

A convenient real-time technique for visualization of the larger arteries and veins by transcutaneous means would be valuable both as a first step in transcutaneous blood flow measurements and as a procedure by itself performed to evaluate the condition of vessels. Accurate quantitative blood flow measurements could be performed with a suitable transcutaneous ultrasonic flowmeter since vessel location, size, and orientation could be reliably determined with the visualization system. By itself, the imaging technique would aid in the diagnosis of several vascular disorders since lumen size could easily be measured to locate constrictions along the vessel length. In addition, a system with adequate resolution would allow changes in the diameters of arteries during the cardiac cycle to be measured. From these changes an estimate of vessel distensibility could be derived.

Transcutaneous visualizations of vessels using ultrasonic Doppler techniques have been reported in the literature, but these operations involved [1,2] multiple scans by a single transducer or transducer pair. Other work[3] with a single pulse-echo transducer generated real-time A-scans across vessels, but relied on specular reflections off the vessel walls to determine vessel size. Not only are such specular reflections inconveniently sensitive to transducer alignment, but the blood-tissue interface within diseased vessels may be difficult to locate using simple pulse-echo techniques under even optimal conditions. Methods utilizing Doppler techniques respond only to moving targets, so delineation of the volumes actually containing flow is possible. However, these scans should be accomplished in real time to permit convenient examination and reduce susceptibility to motion artifact.

The physical constraints that allow the arterial scanner to play a crucial role in the transcutaneous measurement of blood flow are determined by substituting the Doppler relation into the equation for volume flow, Q (in ml/sec) through a lumen of area A.

$$Q = \left(\frac{c}{2 f_o}\right) \frac{1}{\cos \theta} \langle \Delta f \rangle A \qquad (1)$$

where c/f_o is the ultrasonic wavelength, θ is the angle between the average flow vector and the ultrasonic beam path, and $\langle \Delta f \rangle$ is the spatial average Doppler shift measured across the lumen. Of the four factors involved in Q, only the first, ultrasonic wavelength, is known a priori. The average Doppler shift $\langle \Delta f \rangle$ must be measured quantitatively using an appropriate Doppler flowmeter, while the direction cosine and area can be determined by a visualization of the vessel volume containing flow.

Figure 1 shows the transducer array configuration that was developed to use the arterial scanning system in the transcutaneous measurement of blood flow.

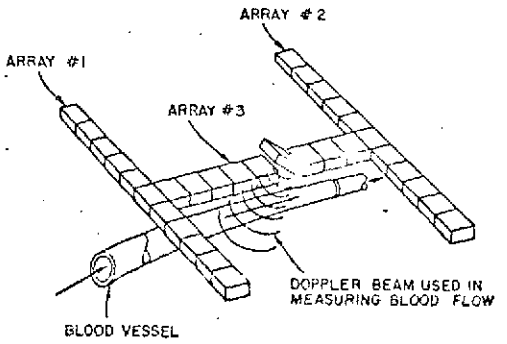

Figure 1. H-array of Transducers.

Three linear arrays of transducer elements are combined to form an H-shaped probe that is placed flat against the skin of the vessel that is being examined. The probe is meant to be aligned so that the cross-bar of the H is directly over the projection of the vessel axis on the skin surface. Each of the transducer elements that are shown in the figure to be flat against the skin are part of the arterial imaging system. The range-gated processor examines a number of depth increments under each transducer element in order to make a qualitative judgement as to whether flow exists at these points or not. The single transducer element that is shown in the figure to be tilted away from the skin surface is not part of the imaging system per se but is used to make a quantitative measurement of the average Doppler shift across the lumen.

Figure 2 illustrates the orthogonal real-time displays of the vessel that are generated by the arterial scanning system when the probe is properly aligned. The parallel segments of the H-array generate scans of the vessel cross section; when each image is centered on the middle row of its display, the probe is properly aligned, and the lumen area can be estimated from these cross-sectional images. The orientation of the lengthwise scan image, generated by array #3, the cross-bar of the H, indicates the angle of the blood velocity vector with respect to the skin. In this way the arterial scanner measures two of the three quantities that must be measured to estimate volume blood flow.

$\left(\frac{1}{\cos\theta}\right)$ and A. The third quantity, the average Doppler shift (Δf) is measured by the single canted transducer element.

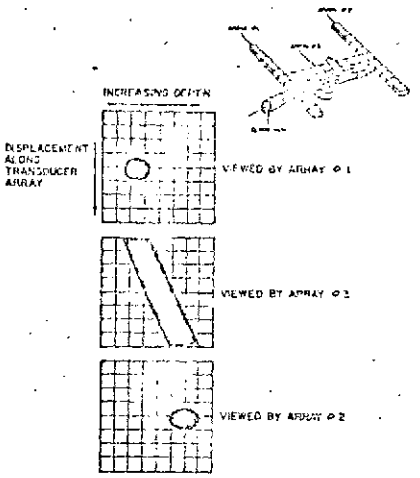

Figure 2. Visualizations Generated by H-array.

Figure 3 shows a simple block diagram of the processor associated with each one of the th linear arrays in the H-shaped probe. The simplest processor utilizing this scheme uses linear audio filters and is not capable of distinguishing flow direction. A later version utilizes an off-set frequency technique and zero-crossing detector to allow determination of flow direction.

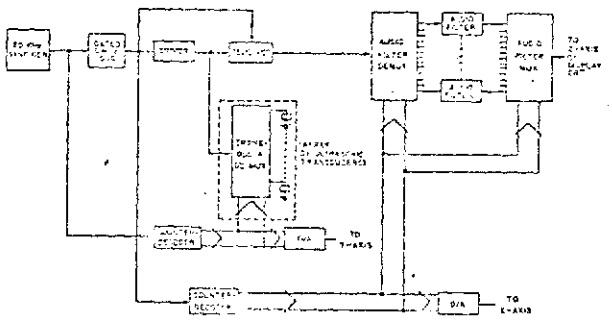

Figure 3. Block Diagram of Doppler Imaging Processor.

The simpler system, using linear audio filters, operates as follows. Every 50 microseconds the driver generates a 1 μsec burst of 6 MHz sinusoid. This signal passes through the transducer multiplexer to a single one of the transducer elements. The reflected ultrasonic signal, detected by the same element, returns through the transducer multiplexer to the Doppler receiver. Here the returning signal is mixed with the local oscillator output, and the resulting video is range gated through a demultiplexer to an audio filter bank. Each of these audio bandpass filters is used to detect a Doppler shifted reflection from a particular depth under the transducer currently being pulsed, while the level of the shift detected modulates the CRT intensity. At any given time the state of the audio filter multiplexer determines the x-displacement of the CRT trace. Since the entire audio filter bank is sequenced beginning with each transmitted pulse, the scope trace covers the entire horizontal axis every 50 μsec. Likewise at any given time the state of the transducer multiplexer determines the y-displacement of the trace.

Each transducer element is activated for 10 msec before the multiplexer is stepped if Doppler shifts as low as 100 Hz are to be detected. The scope trace is then also stepped in the y-direction every 10 msec; with 10 transducer elements in an array we then achieve 10 frames per second.

The later processing system capable of distinguishing flow direction operates similarly. However, in this case the reflected signal is mixed with a frequency offset by 4 kHz from the drive frequency. Also, instead of a linear audio filter bank, a bank of zero-crossing detectors and counters is used. During the 10 msec a particular transducer is being pulsed, counters indicating less than 39 counts indicate flow away from the transducer, and counts greater than 41 indicate flow toward the transducer.

The first H-array to be assembled contains a total of 39 element pairs. Each element pair is in turn multiplexed to a hybrid transformer scheme allowing common-mode drive and differential receive configurations. The element pair dimensions in the cross-arrays are 1.5 mm × 3 mm, while those in the lengthwise array are 2 mm × 3 mm. The transducer material is LTZ-2, utilizing an energy absorptive backing and quarter-wave transformer layer to increase transducer bandwidth.

The transducer multiplexer now used is assembled from commercial JFET components capable of switching 20 volts peak to peak; when these are replaced by higher voltage devices, more power can be delivered to the far end of the transducer Fresnel zones. This capability will allow penetration of the layers of fat and muscle that cover vessels like the carotid artery system. In this way routine real-time scans of these and other important arteries can be made, and transcutaneous measurements can be made of the flow through these vessels.

Acknowledgement

This investigation was supported by PHS Research Grant No. 1P01 GM17940-03 from the Department of Health, Education, and Welfare, and by NASA Research Grant No. NGR 05-020-015.

References

1. Mozersky, D.J., et al., "Ultrasonic Arteriography", Arch. Surg., Vol. 103, Dec. 1971, pg. 663.

2. Reid, J.M., Spender, M.P., Science, Vol. 176, 16 June 1972, pg. 1235.

3. Masterson, J.E., et al., "Ultrasonic Echography for Direct Observation of Peripheral Arteries", Vascular Diseases, April 1966, pg. 109.

2. Doppler Spectrum First Moment Detector (Levy Gerzberg)

To measure blood flow, the average velocity of blood particles in the cross-section area, the lumen, of the vessel needs to be measured. It can be shown that, in the case of uniform illumination, of the blood vessel with the ultrasonic beam, the average velocity is proportional to the normalized first moment of the Doppler power spectrum of the returned signal. The $\sqrt{\omega}$ - type first moment detector was found to be the optimal demodulator for use with the various types of Doppler flowmeters. This detector was first simulated on a digital computer for optimal system design and then was built with commercially available discrete components. With the aid of computer-aided design (CAD) many more alternatives could be considered than would have been possible if each had had to be physically constructed. The accuracy of the detector was found to be 2% with a single-frequency input signal and 5% with a wide-band signal of 18 dB signal-to-noise ratio. In the future a monolithic form of the first-moment detector will be developed.

As a first step in the development of the monolithic form of this detector, CAD has also been used. The computer is being used both for the simulation of models for some of the devices used in the detector and for optimal design of the integrated circuit when processing limitations and parasitic effects are taken into account.

C. Implementation Techniques (W. R. Freund)

The study to determine a valid calibration scheme for measurement of blood flow in the renal and iliac arteries has continued. Telemetered information has been collected from eleven animals during periods of rest and excercise. These data will be summarized and analyzed to establish the normal range and velocities which can be expected for renal and iliac flows in unanesthetized canines. Arteriograms have been completed on four of these animals to measure the vessel lumen area and the amount of occlusion produced by the small-vessel CW cuffs. The diameters of the three left and one right renal artery range in value from 2.5 to 3.0 mm with a mean diameter of 2.75 mm. The diameters of the four iliac arteries ranged in value from 2.9 to 4.3 mm with a mean diameter of 3.55 mm. In one of the animals a significant occlusion was produced by an additional CW cuff placed on the right renal artery. The lumen was measured to be less than one mm in diameter as a result. While the kidney appeared to be well perfused and free from infarcts, pressure cathether measurements showed that the animal was severely hypertensive. A direct bleedout calibration produced maximum volume flows of 90 ml/min (approximately 1/3 the expected flow for the 20 kg animal). Post-mortem examination revealed that the occlusion was due to an incorrect choice of cuff size rather to excessive formation of scar tissue. With the exception of this case, no vessel occlusion has been observed.

The development of special purpose measurement techniques has continued. Three specific applications have been investigated: (1) The measurement of coronary blood flow with the existing CW, small vessel flow cuffs, (2) The measurement of coronary blood flow with existing pulsed doppler equipment, and (3) The measurement of aortic flows with a catheter-tip, doppler transducer.

Initial attempts to use the existing CW small-vessel cuffs in the measurement of coronary velocities have been unsuccessful. A new version has been designed which would be optimized for the measurement of coronary flow. This new transducer assembly will be constructed and tested in the near future.

Acute studies have deomonstrated the difficulties involved in using pulsed flowmeters and transducers to measure flow in very small vessels such as the coronary arteries. These problems arise partly from the relatively long wavelength of the six megahertz ultrasound in comparison to the size of the coronary lumen. Experiments are continuing

to determine those combinations of transducers, construction and excitation frequency that would facilitate the measurement of coronary blood flow by pulsed Doppler flowmeters.

A concurrent effort has been initiated to combine an SEL directional flowmeter and a commercially available, catheter tip, transducer produced by Southwest Research Institute, San Antonio, Texas. This catheter, positioned by use of X-ray techniques, could be used for (1) relatively non-invasive measurements of velocities in the major blood vessels prior to (or in place of) implantation of a more complicated telemetry system, (2) comparison with previously implanted electromagnetic flowmeters to establish a non-occlusive "flow zero" (3) comparison with previously implanted non-directional Doppler flow meters to add directional information, and (4) comparison with waveforms produced by transcutaneous Doppler flowmeters.

The first waveforms collected are shown in the figure, below. Information was recorded while the catheter was positioned along the axis of flow in the descending aorta. Research on this technique will continue.

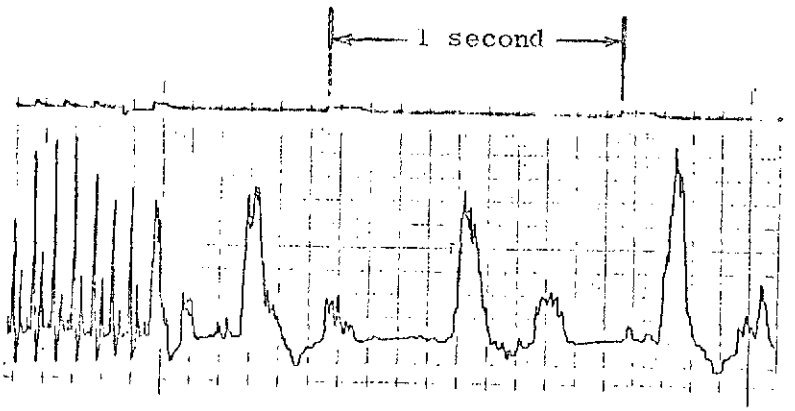

Velocity in the Descending Aorta -- Catheter-tip Doppler

III. CONCLUSIONS

Sample implantable flowmeter designs, suitable for use with a dog aorta, human aorta, human renal artery and human coronary artery, are tabulated at the end of Section A, on the Implantable Pulsed Flowmeter, together with a figure of merit for each, indicative of the degree of precision in measurement technique possible, and the way in which this is dependent on physiological constraints. Future work in this area will be directed toward confirmation of these designs in actual construction and tests.

For transcutaneous observation of blood flow, several systems have been designed. One design concept, the H-array, has been constructed and tested satisfactorily using target specimens in a water tank. Lumen area and vessel orientation can be determined by this means. This information, combined with Doppler information from the returned echoes enables calculation of flow volume. Two simplified new concepts have been developed recently, which avoid the need to determine vessel orientation. The simpler of these will be constructed during the next year. It will have a single linear array for visualization and a separate transducer to produce uniformly distributed sound for use in measuring the first moment of the Doppler spectrum. When the velocity distribution is not symmetrical across the lumen, the first moment of the Doppler spectrum is the only type of average measurement that reflects accurately the true velocity.

Technique development for implementing flowmeter use resulted in success with CW flowmeters but some problems with pulsed flowmeters on small vessels. Higher frequency sound, than the current 6 MHz, will also be needed for satisfactory operation of the pulsed Doppler flowmeters on small vessels. Its shorter wavelength should permit more accurate observations to be made, but several design criteria must be modified as a result.